3622 © 1989 The Chemical Society of Japan Bull. Chem. Soc. Jpn., 62, 3622—3627 (1989) [Vol. 62, No. 11

Kinetic Study on Hydrogenation of Isoquinoline over Supported Ruthenium Catalysts

Hiroshi Okazaki,* Mahito Soeda, Yoshio Ikefuji,† Ryuji Tamura,† and Isao Mochida††
R&D Laboratories, Nippon Steel Chemical Co., Tobataku, Kitakyushushi 804
†Technical Part, Iwatani Industrial Gases Corp., Yodogawaku, Osakashi 532
††Research Institute of Advanced Material Study, Kyushu University,
Kasugashi 816

(Received May 11, 1989)

The hydrogenation of isoquinoline (**1**) to isomeric decahydroisoquinoline (**4**) via 1,2,3,4-tetrahydroisoquinoline (**2**) or 5,6,7,8-tetrahydroisoquinoline (**3**) was kinetically studied over supported ruthenium catalysts under 50—100 atm hydrogen pressure at 135—170 °C. The results showed that the reaction proceeds mainly via **2** over ruthenium on carbon, and via **2** and **3** competitively over ruthenium on alumina. Such reaction features are explained from the view points of their adsorption and the activation of the molecules on the catalysts based on quantum chemical indices. The acidic nature of alumina support exhibited a preference of nitrogen lone-pair defining the adsorption of substrates, and consequently influencing on the reaction route. The proposed approach distinguished the present catalyst from Raney nickel examined in a previous paper. The noble and base metals may interact differently with the substrate, although both metals are classified as "soft".

In a previous paper,[1)] we reported the selective preparation of some useful hydroisoquinolines using several commercial catalysts. Raney nickel (R-Ni) promoted the following consecutive reactions: **1**→**2**→**3**→**4** (cis) →**4** (trans).[2)] On the other hand, a preliminary examination of a ruthenium catalyst suggested that **1** was rapidly hydrogenated to the cis- and trans-isomers of **4** via **2** and **3** simultaneously. The isomeric mixture of **4** is a starting material to perfluoro (*N*-methyldecahydroisoquinoline), an oxygen carrier for medical use.[3)] Therefore, it is practically important to clarify the kinetics and mechanism of hydrogenation of **1** over ruthenium catalysts to control the product selectivity.

In the present work, the hydrogenation of **1** was studied kinetically in detail using ruthenium on carbon (Ru/C) and on alumina (Ru/Al_2O_3). Such a study may allow discussion on the reaction pathways for the hydrogenation of **1**, and on the adsorption and activation of substrates over ruthenium catalysts, both of which are expected to be entirely different from those over R-Ni. The structural factors of the substrates which influence strongly on their adsorption and activation are discussed by a semiempirical molecular orbital calculation.

Experimental

Materials. Isoquinoline was used after purification of commercial grade material produced from coal tar. Two tetrahydrogenated isomers were separated from the hydrogenated isoquinoline. Both procedures were described in the previous papers.[1,2)] No sulfur-containing contaminant was found in all substrates. Ru/C was purchased from Nippon Engelhard Ltd. in dry state. Ru/Al_2O_3 was purchased from Nikki Chemical Co. in wet state (water content is about 50 wt%) and used without drying. Their ruthenium contents were 5 wt% on the dry base.

Hydrogenation Procedure and Analytical Method. 100 g of a starting material was hydrogenated over ruthenium catalyst in a 200 ml-autoclave with stirring at a constant pressure and temperature. The reaction conditions for three starting substrates (**1**, **2**, and **3**) were as follows; temperature range: 135—170 °C, hydrogen pressure range: 50—100 atm, amount of Ru/C or Ru/Al_2O_3 catalysts: 4 wt% in dry state per substrate (see Table 2 for the detailed conditions). The reaction mixture was sampled at appropriate times, and was diluted to 5 ml with methanol. After filtering off the catalyst, the product was analyzed by gas chromatography as described previously.[2)] **4** contained two isomers, of which cis/trans ratio ranged from 2 to 4. The compounds other than **1**—**4** were less than 5% in all of the reactions.

Quantum Chemical Calculation. Quantum chemical indices of isoquinoline and its derivatives were obtained by the MNDO-MO[4)] calculation using a CRAY X-MP/216 computer.[5)] The geometries of all of the molecules were energetically optimized with the flat configuration of aromatic rings.

Results

Kinetic Modeling. Some kinetic models were tested, and the network shown in Fig. 1 and the following Langmuir-Hinshelwood type rate equations[2,6—8)] were found to fit with our experimental data. This network contains the isomerization of **2** to **3**, but neither

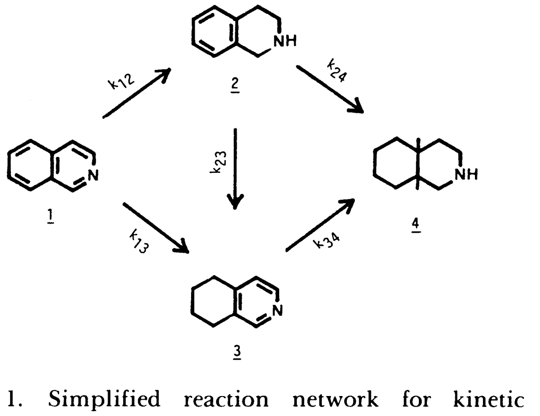

Fig. 1. Simplified reaction network for kinetic analysis.

dehydrogenation nor cis/trans isomerization of **4** was included, because relatively higher hydrogen pressures, lower temperatures, and shorter reaction times were employed in this work.

$$\frac{dC_1}{dt} = \frac{-m(k_{12}+k_{13})K_1C_1}{1+K_1C_1+K_2C_2+K_3C_3+K_4C_4}, \tag{1}$$

$$\frac{dC_2}{dt} = \frac{m[k_{12}K_1C_1-(k_{23}+k_{24})K_2C_2]}{1+K_1C_1+K_2C_2+K_3C_3+K_4C_4}, \tag{2}$$

$$\frac{dC_3}{dt} = \frac{m[k_{13}K_1C_1+k_{23}K_2C_2-k_{34}K_3C_3]}{1+K_1C_1+K_2C_2+K_3C_3+K_4C_4}, \tag{3}$$

and

$$\frac{dC_4}{dt} = \frac{m[k_{24}K_2C_2+k_{34}K_3C_3]}{1+K_1C_1+K_2C_2+K_3C_3+K_4C_4}, \tag{4}$$

where C_i is the concentration of species i (the initial value of isoquinoline, $C_1(t=0)$, was 8.52 mol dm^{-3} under STP conditions), t is the reaction time (h), m is the concentration of catalyst (g dm^{-3}), k_{ij} is the apparent rate constant of reaction $i \rightarrow j$ (the constant is a function of hydrogen pressure), and K_i is the equilibrium adsorption constant of species i. In contrast to the case of the R-Ni catalyst,[2] absolute values of K_i were calculated in this study, because unity in the denominator of Eqs. 1—4 was not neglected on the ruthenium catalysts.

Equilibrium Adsorption Constants and Rate Constants. K_i and k_{ij} in the above equations were determined by a curve fitting procedure. It was assumed that each value of K_i is constant under the present expreimental conditions when the same catalyst is used. The theoretical product distributions were calculated by a numerical analysis containing the Runge-Kutta-Gill routine. The values of K_i and k_{ij} were determined with the degree of agreement between experimental product distributions and the respective theoretical values. First, K_3, K_4, and k_{34} were determined by the Eqs. 3 and 4 and the data obtained from the experiment in which **3** was employed as the starting material. Secondly, K_2, k_{23}, and k_{24}, were determined with the above values of K_3, K_4, and k_{34}, the Eqs. 2—4 and the data obtained from the experiment in which **2** was employed as the starting material. Thirdly, K_1, k_{12}, and k_{13} were determined in a similar manner to the above. Figures 2—7 show some example of the product distributions on the hydrogenation of **1**, **2**, and **3** over Ru/C or Ru/Al_2O_3. The calculated values (solid lines) are in good agreement with the experimental data (dots). Their presisions of simulation were about ±5%. It is noticed during the

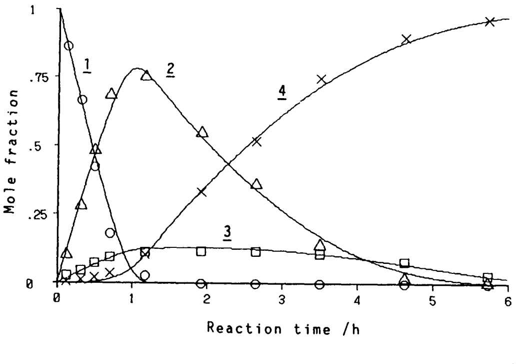

Fig. 2. Product distributions on the hydrogenation of **1** over Ru/C at 150 °C under 100 atm H_2 pressure. **1**: isoquinoline, **2**: 1,2,3,4-tetrahydroisoquinoline. **3**: 5,6,7,8-tetrahydroisoquinoline, **4**: decahydroisoquinoline.

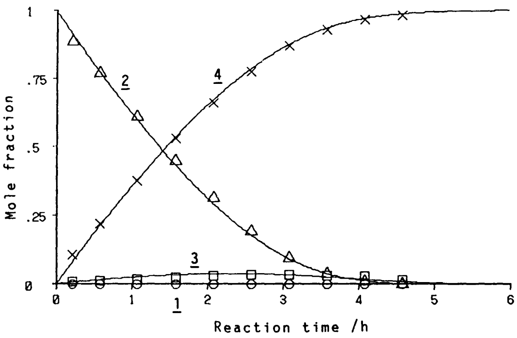

Fig. 3. Product distributions on the hydrogenation of **2** over Ru/C at 145 °C under 100 atm H_2 pressure. See Fig. 2 for the chemical names of symbols.

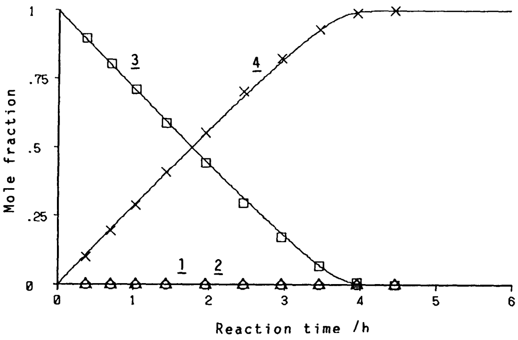

Fig. 4. Product distributions on the hydrogenation of **3** over Ru/C at 170 °C under 100 atm H_2 pressure. See Fig. 2 for the chemical names of symbols.

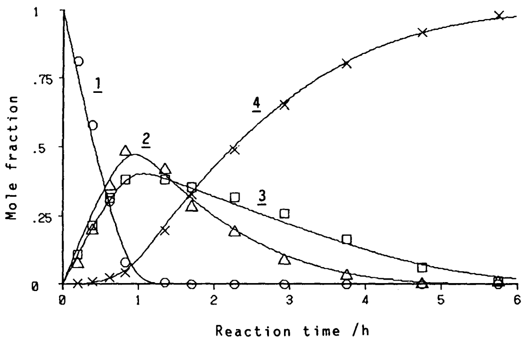

Fig. 5. Product distributions on the hydrogenation of **1** over Ru/Al_2O_3 at 150 °C under 100 atm H_2 pressure. See Fig. 2 for the chemical names of symbols.

hydrogenation of **1** that the composition of **3** over Ru/Al$_2$O$_3$ (Fig. 5) was considerably higher than that over Ru/C (Fig. 2).

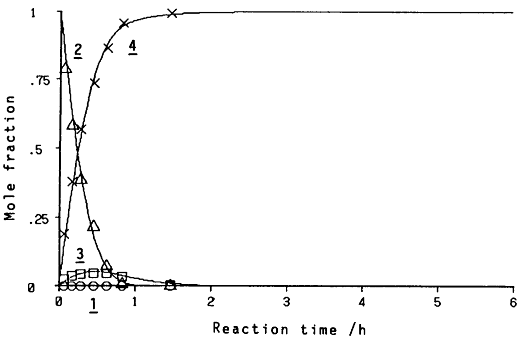

Fig. 6. Product distributions on the hydrogenation of **2** over Ru/Al$_2$O$_3$ at 157 °C under 100 atm H$_2$ pressure. See Fig. 2 for the chemical names of symbols.

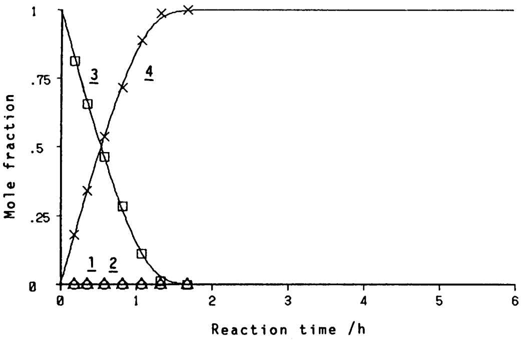

Fig. 7. Product distributions on the hydrogenation of **3** over Ru/Al$_2$O$_3$ at 165 °C under 100 atm H$_2$ pressure. See Fig. 2 for the chemical names of symbols.

Table 1. Equilibrium Adsorption Constants

Catalyst	K_1	K_2	K_3	K_4
	dm^3 mol^{-1}			
Ru/C	35.0	2.3	7.0	0.12
Ru/Al$_2$O$_3$	70.0	4.7	14.1	1.8

Table 1 summarizes the values of K_i. The precision of constants K_i was about ±50%. The relative values of K_i/K_1 over the ruthenium catalysts are different from that over R-Ni reported previously.[2] The respective relative values except for K_4/K_1 were much the same over Ru/C and Ru/Al$_2$O$_3$.

Table 2 summarizes the values of k_{ij}. The precision of the constants was about ±20%. The value of k_{13} over Ru/Al$_2$O$_3$ is much larger than that over Ru/C. Roughly linear relations of the constants against hydrogen pressure were observed at 150 °C over Ru/C as shown in the table.

The effects of temperature on rate constants of all steps over Ru/C under 100 atm of hydrogen pressure are shown in Fig. 8. The apparent activation energy of

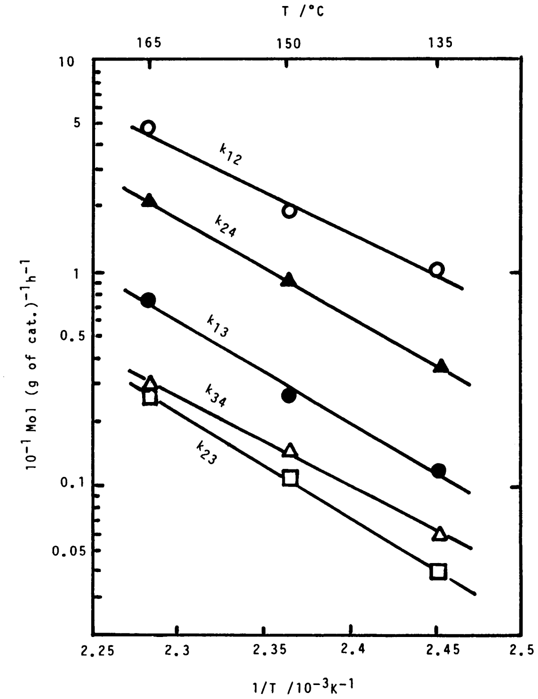

Fig. 8. Arrhenius plot for hydrogenation of isoquinoline over Ru/C under 100 atm H$_2$ pressure.

Table 2. Rate Constants on Hydrogenation of Isoquinoline and Partial Hydroisoquinolines over Ruthenium Catalysts

Run No.	Cat.[a]	Starting material[b]	Press.	Temp.	k_{12}	k_{13}	k_{23}	k_{24}	k_{34}
			atm	°C	10^{-1} mol (g of cat.)$^{-1}$ h^{-1}				
1	Ru/C	**1**	100	135	1.05	0.12	0.04	0.37	0.06
2		**1**	100	150	1.94	0.27	0.11	0.95	0.15
3		**1**	100	165	4.84	0.76	0.27	2.23	0.31
4		**1**	50	150	1.06	0.16	0.07	0.48	0.07
5		**2**	100	145			0.06	0.77	0.12
6		**3**	100	170					0.56
7	Ru/Al$_2$O$_3$	**1**	100	150	1.37	1.06	0.17	1.94	0.33
8		**2**	100	157			0.43	4.65	0.62
9		**3**	100	165					1.94

a) The amount of catalyst is 4wt% on dry base. b) **1**; isoquinoline, **2**; 1,2,3,4-tetrahydroisoquinoline, **3**; 5,6,7,8-tetrahydroisoquinoline.

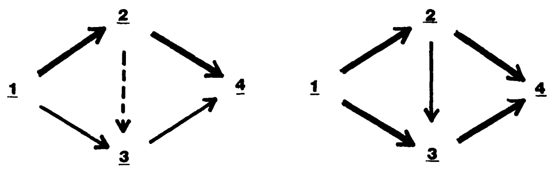

(a) over Ru/C, (b) over Ru/Al_2O_3.

Fig. 9. Reaction pathways on hydrogenation of isoquinoline. (a) over Ru/C, (b) over Ru/Al_2O_3.
➡; major ⟶; minor - - →; rare

step 2→4 over Ru/C was calculated to be 20±4 kcal mol^{-1} from the gradients of lines in the figure. It is recognized that the barrier of step 2→4 over Ru/C is lower than over R-Ni(about 60 kcal mol^{-1}).[2)]

Dominant Reaction Routes. As the result of above analyses, the dominant routes in hydrogenation of **1** to **4** were determined as illustrated in Fig. 9. The reaction proceeds mainly via **2** over Ru/C, and competitively via **2** and **3** over Ru/Al_2O_3. The isomerization of **2** to **3** is very minor and the hydrogenation of **2** to **4** proceeds readily on both ruthenium catalysts in contrast to R-Ni catalyst. The rates of each step except **1**→**2** over Ru/Al_2O_3 are larger than those over Ru/C.

Quantum Chemical Calculation. Table 3 summarizes quantum chemical indices of isoquinoline and its tetrahydrogenated derivatives. Some notable conclusions are as follows: The calculations appear to reproduce the thermodynamic stability of substrates and products. The total energy and energy levels of frontier orbitals indicate that **1** is stabilized by hydrogenation, and that **2** is more stable than **3**. The electronegativity of N-atom localizes more π-electrons in pyridine ring than benzene ring of **1**. The degree of localization is decreased by the hydrogenation of pyridine or benzene ring of **1**. A similar trend of localization is also noted for π-bond orders.

Discussion

The kinetic anlysis of the present study revealed that ruthenium catalysts have some contrast features is the catalytic hydrogenation of isoquinoline to those of R-Ni in the previous studies.[1,2)] The catalytic reactions on ruthenium catalysts proceeded in two consecutive routes of **1**→**2**→**4** and **1**→**3**→**4**. The selectivity between the two routes depends upon the supports, carbon or alumina.

Products of **2** and **3** were not further hydrogenated into **4** before almost all of **1** disappeared on the Ru catalysts, while the product retardation indicating stronger adsorption of **2** was observed on R-Ni as previously reported.[2)] Such reaction features of the ruthenium catalyst reflect on the equilibrium adsorption constants shown in Table 1. Strong adsorption of **1**, moderate one of **2** and **3** and very weak one of **4** are clearly indicated in the table. In spite of slightly stronger adsorption of **3**, **2** competes with **3** for the active sites for further hydrogenation to **4**, probably due to different concentrations of active sites which reflect on the selectivity.

Such a trend of adsorption strength is completely different from that on R-Ni, which is appreciably related to the pK_a values of the substrates.[1)] Although nitrogen heterocyclic compounds such a pyridine and isoquinoline have been widely believed to be vertically adsorbed at their nitrogen lone pair onto the metal surfaces[9,10)] as postulated on R-Ni,[2)] the aromatic π-electrons can also contribute to the adsorption on metals such as ruthenium which is classified as a "soft" metal.[11)] Such π-coordination[12,13)] appears to play a major role in defining the trend of adsorption strength on the present noble catalysts.

The equilibrium adsorption constants over the present catalysts will be relevant in first approximation to their number of π-electrons. It is obvious that adsorption of **4** is very weak due to the absence of π-electron. The minor difference betweeen **2** and **3** of the same π-electron number may be ascribed to slightly more localization of π-electron on the nitrogen atom of the substrate **3** according to the quantum chemical calculation. It has been pointed out that the back donation from the metal to the substrate contributes strongly to the adsorption of unsaturated substrate.[14)] The energy level of LUMO can be an index for the degree of the back-donation. Substrates **1**, **3**, and **2** show a rising order of energy level of their LUMO as shown in Table 3, corresponding again to the order of their adsorption constants.

Such an adsorption through π-electrons in the aromatic ring defines the adsorption form of **1** to be flat to the surface. The heterocyclic ring which is more reactive as discussed later is preferentially hydrogenated to produce **2**. However, some chance of hydrogenation of benzene ring may also exist to produce **3** especially when the hydrogenation of heterocyclic ring is hindered by some reason. The latter hydrogentation is very difficult on R-Ni, where the substrate seems to be adsorbed vertically at its nitrogen atom in the direction of lone-pair.[2)]

The rate constant of the hydrogenation on Ru/C decreased in the order of $k_{12}>k_{24}>k_{34}$. The reactivity of the substrate appears to be related primarily to the π-bond order, which reflects the degree of unsaturation. The highest unsaturation leads to the highest reactivity to hydrogen. The highest value of π-bond order in the substrate **1** is 0.79 and the value is higher than those of **2** and **3**. The energy level of electron donating HOMO may also contribute to the reactivity in such a reaction, the order of substrates **1**, **2**, and **3** corresponds to their reactivity order.

The rate constants k_{13} and k_{13} define the intramolecular selectivity within the substrate **1**. The π-bond

Table 3. Several Quantum Chemical Properties of Isoquinoline and Its Tetrahydrogenated Compounds Calculated by MNDO Method

	Isoquinoline			1,2,3,4-Tetrahydro-			5,6,7,8-Tetrahydro-		
[Total energy[a] and frontier orbital energy/eV]									
	Total	HOMO	LUMO	Total	HOMO	LUMO	Total	HOMO	LUMO
	−1455.86	−8.89	−0.59	−1513.63	−9.34	0.22	−1514.01	−9.66	−0.03
[Total and frontier electron density]									
Atom[b]	Total	HOMO	LUMO	Total	HOMO	LUMO	Total	HOMO	LUMO
1	3.910	0.236	0.377	3.838			3.933	0.431	0.124
2	5.231	0.035	0.099	5.333			5.229	0.003	0.143
3	3.961	0.297	0.170	3.890			3.947	0.473	0.612
4	4.102	0.370	0.337	3.962			4.112	0.400	0.053
5	4.053	0.349	0.343	4.047	0.001	0.000			
6	4.037	0.061	0.164	4.055	0.420	0.482			
7	4.066	0.267	0.151	4.059	0.416	0.399			
8	4.020	0.319	0.358	4.043	0.002	0.009			
9	3.999	0.040	0.000	4.063	0.491	0.486	4.020	0.015	0.326
10	4.108	0.027	0.000	4.079	0.503	0.555	4.137	0.588	0.679
[Total and frontier π-bond orders]									
Bond[b]	Total	HOMO	LUMO	Total	HOMO	LUMO	Total	HOMO	LUMO
1—10	0.471	0.080	0.002				0.638	0.503	−0.290
1—2	0.791	0.091	−0.194				0.675	−0.037	0.133
2—3	0.523	−0.102	0.130				0.658	0.039	−0.295
3—4	0.785	0.332	−0.239				0.658	0.435	−0.179
4—9	0.493	−0.122	−0.006				0.662	0.092	0.131
9—5	0.490	0.118	0.006	0.656	0.021	0.015			
5—6	0.797	0.145	−0.237	0.673	−0.019	−0.015			
6—7	0.515	−0.127	0.157	0.659	0.418	−0.439			
7—8	0.796	0.292	−0.232	0.673	−0.025	0.061			
8—10	0.494	−0.093	−0.002	0.657	0.027	−0.072			
9—10	0.624	0.033	−0.000	0.655	0.497	−0.519	0.663	−0.093	−0.470

a) The sum of electron energy and core repulsion energy. b) The numbering is as follows;

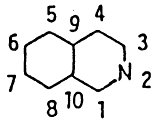

order in HOMO is largest between atoms 3 and 4, probably contributing to the larger reactivity of its pyridine ring, although the largest π-bond orders (total) in the benzene and pyridine rings of substrate **1** are similar. According to the correlations described above, the hydrogenation reaction may be initiated by the addition of hydrogen radical to one of the unsaturated bonds in pyridine ring of **1** over Ru/C, successive hydrogenation being rapid to complete saturation of the ring.

According to the kinetic analyses, the isomerization step of **2**→**3** was very slow in comparison with the rates of major hydrogenation reactions on the ruthenium catalysts. The substrate **2** of which adsorption was not so strong on ruthenium may not find a time to isomerize before its rapid hydrogenation into **4**.

Catalyst supports for ruthenium play some interesting roles in defining the selectivity in the present catalyic hydrogenation even if Ru behaves as a soft metal on both supports. First point is that Ru/Al_2O_3 produced comparable amounts of **2** and **3**, while Ru/C gave **2** preferentially. The presence of Brønsted acids was reported to exclude the hydrogenation of heterocyclic ring of **1**.[15,16] The protonation modifies significantly the reactivity indices of isoquinoline as shown in Fig. 10. The modified regioselectivity against hydrogenation may be explained by the π-bond orders in HOMO of the protonated substrate of **1**. A significant increase of the π-bond order between atoms 7 and 8 and decrease of that between atoms 3 and 4 may cause the change of hydrogenation preference from pyridine to benzene ring. It is therefore

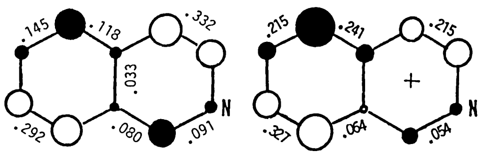

(a) Isoquinoline (b) Isoquinolinium cation

Fig. 10. π-Bond orders in HOMO calculated by MNDO method. (a) Isoquinoline, (b) isoquinolinium cation.

considered that acidity of the catalyst decreases the selectivity of **2** and increases that of **3**, although the contribution of Brønsted acid on the alumina support is not definite and the protonated isoquinoline is a critical model. Much larger equilibrium adsorption constant of highly basic **4** ($pK_a=11.0$) on Ru/Al_2O_3 than that on Ru/C may also reflect acidic natures of the former support, while the constants for other substrates on the former catalyst were only twice larger than those on the latter catalyst.

The second point is concerned with the rate constants of reactions **2**→**3**, **2**→**4**, and **3**→**4**, which were almost twice larger on the Ru/Al_2O_3 than on Ru/C, while the summed rate constants of **1**→**2** and **1**→**3** reactions were identical. However, the differences on rate constants are not discussed in detail.

The dispersion of ruthenium on the supports will be another important factor affecting the catalytic activity, but it is beyond the scope of the present study.

References

1) H. Okazaki, M. Soeda, K. Onishi, and R. Tamura, *Appl. Catal.*, **41**, 99 (1988).

2) H. Okazaki, M. Soeda, Y. Ikefuji, and R. Tamura, *Appl. Catal.*, **43**, 71 (1988).

3) Y. Naito, Y. Inoue, T. Ono, Y. Arakawa, C. Fukaya, K. Yokoyama, Y. Kobayashi, and K. Yamanouchi, *J. Fluorine Chem.*, **26**, 485 (1984).

4) M. J. Dewar, *J. Am. Chem. Soc.*, **99**, 4899 (1977).

5) The name of program is "MOPAC", Ver. 3.1 (QCPE #516); J. J. P. Stewart, *QCPE Bulletin* **6**, (4), 99(1986), Dept. of Chemistry of Indiana University.

6) J. Sonnemans, J. M. Janus, and P. Mars, *J. Phys. Chem.*, **80**, 2107 (1976).

7) Y. S. Shih and S. S. Yang, *J. Catal.*, **79**, 132 (1983).

8) C. N. Satterfield and S. H. Yang, *Ind. Eng. Chem. Process Des. Dev.*, **23**, 11 (1984).

9) C. E. Calf and J. L. Garnett, *Chem. Commun.*, **1967**, 306.

10) C. G. MacDonald and J. S. Shannon, *Tetrahedron Lett.*, **1964**, 3351.

11) R. G. Pearson, *J. Am. Chem. Soc.*, **85**, 3533 (1963).

12) J. L. Garnett and W. A. Sollich-Baumgartner, *Adv. Catal.*, **16**, 95 (1966).

13) R. R. Fraser and R. N. Renaud, *J. Am. Chem. Soc.*, **88**, 4365 (1966).

14) J. Chatt and L. A. Duncanson, *J. Chem. Soc.*, **1953**, 2939; M. J. S. Dewar, *Bull. Soc. Chim. Fr.*, **18**, C79 (1951).

15) J. Z. Ginos, *J. Org. Chem.*, **40**, 1191 (1975).

16) F. W. Vierhapper and E. L. Eliel, *J. Org. Chem.*, **40**, 2729 (1975).